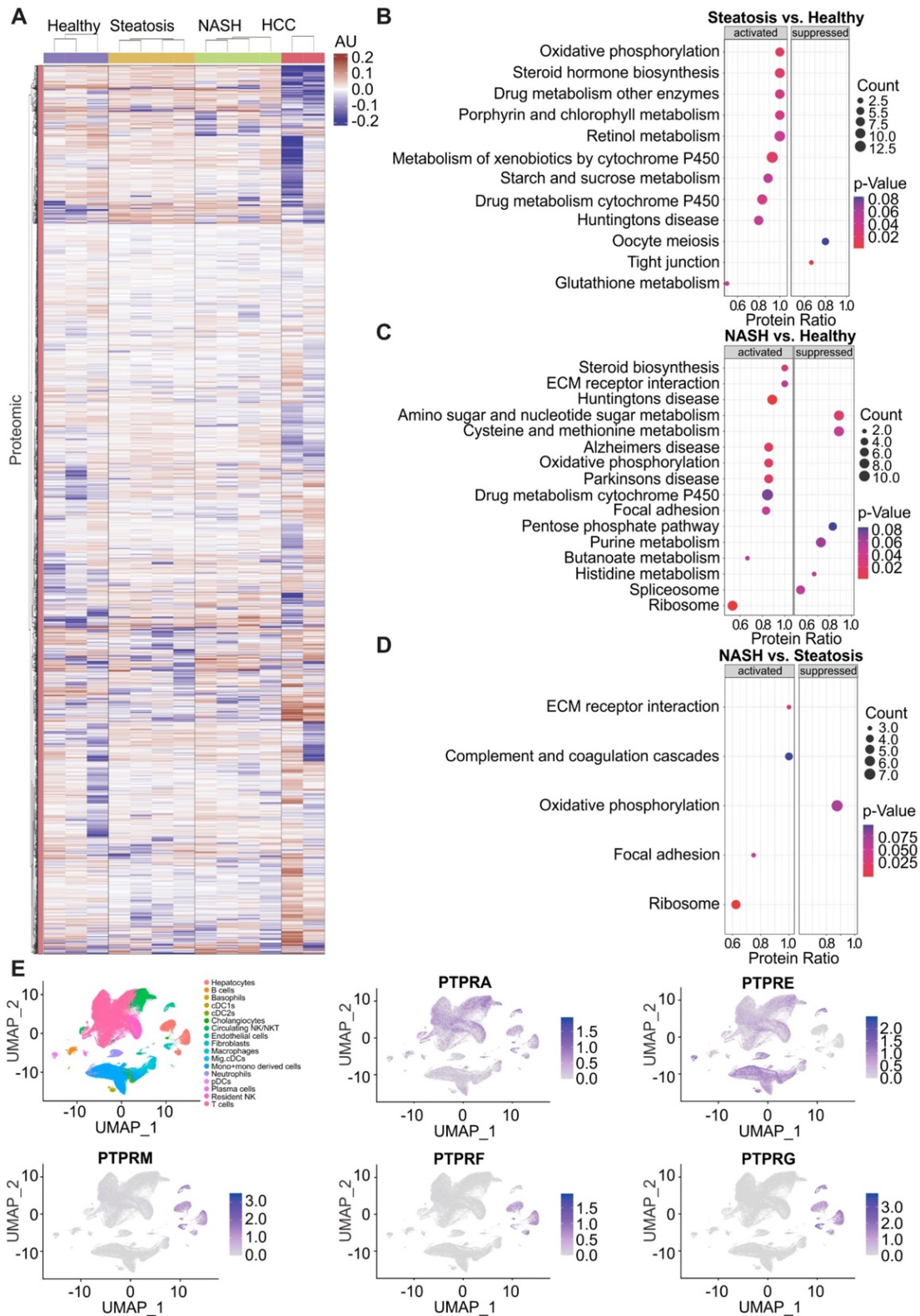


Supplementary information

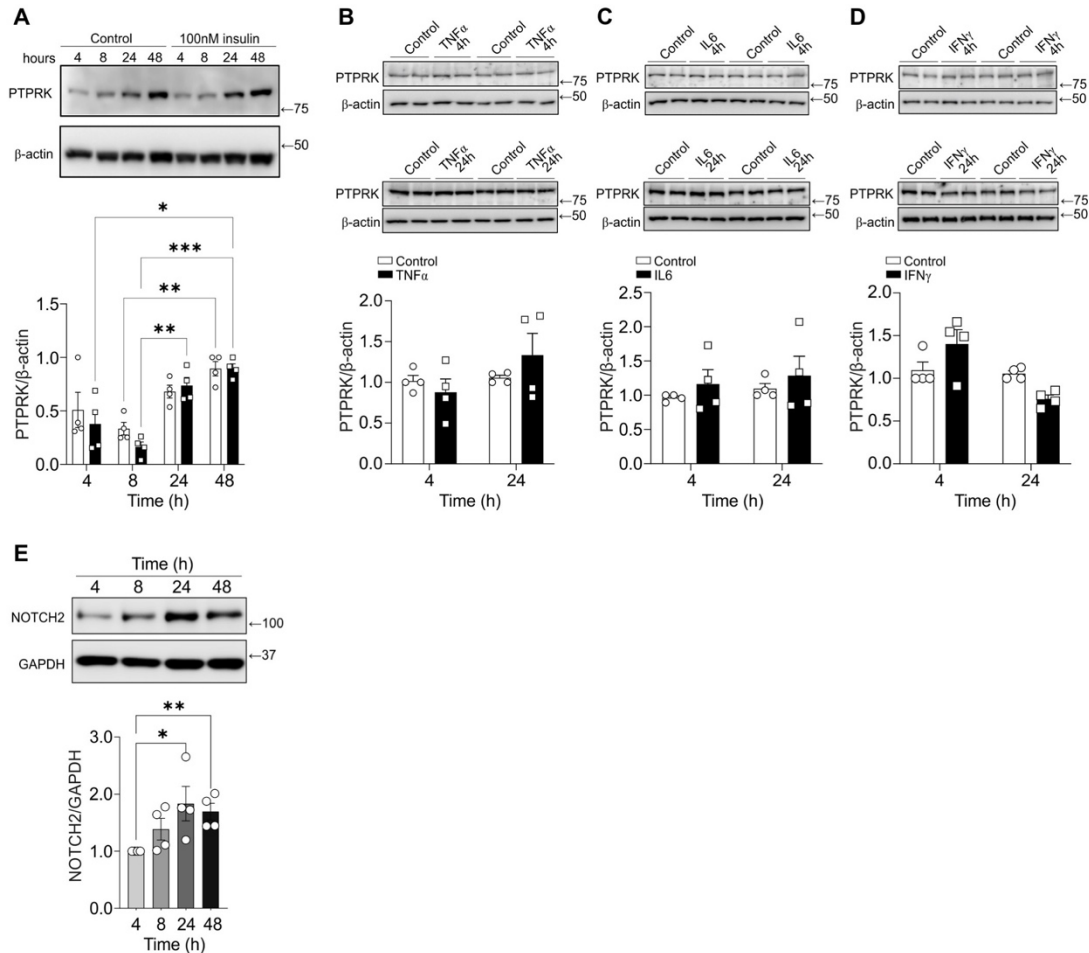
Protein tyrosine phosphatase receptor kappa regulates glycolysis and *de novo* lipogenesis to promote hepatocyte metabolic reprogramming in obesity

Eduardo H. Gilglioni, Ao Li, Wadsen St-Pierre-Wijckmans, Tzu-Keng Shen, Israel Pérez-Chávez, Garnik Hovhannisyán, Michela Lisjak, Javier Negueruela, Valerie Vandenbempt, Julia Bauzá-Martinez, Jose M. Herranz, Daria Ezerina, Stephane Demine, Zheng Feng, Thibaut Vignane, Lukas Otero-Sánchez, Flavia Lambertucci, Alena Prašnická, Jacques Devière, David C. Hay, Jose A. Encinar, Sumeet Pal Singh, Joris Messens, Milos R. Filipovic, Hayley J. Sharpe, Eric Trépo, Wei Wu and Esteban N. Gurzov



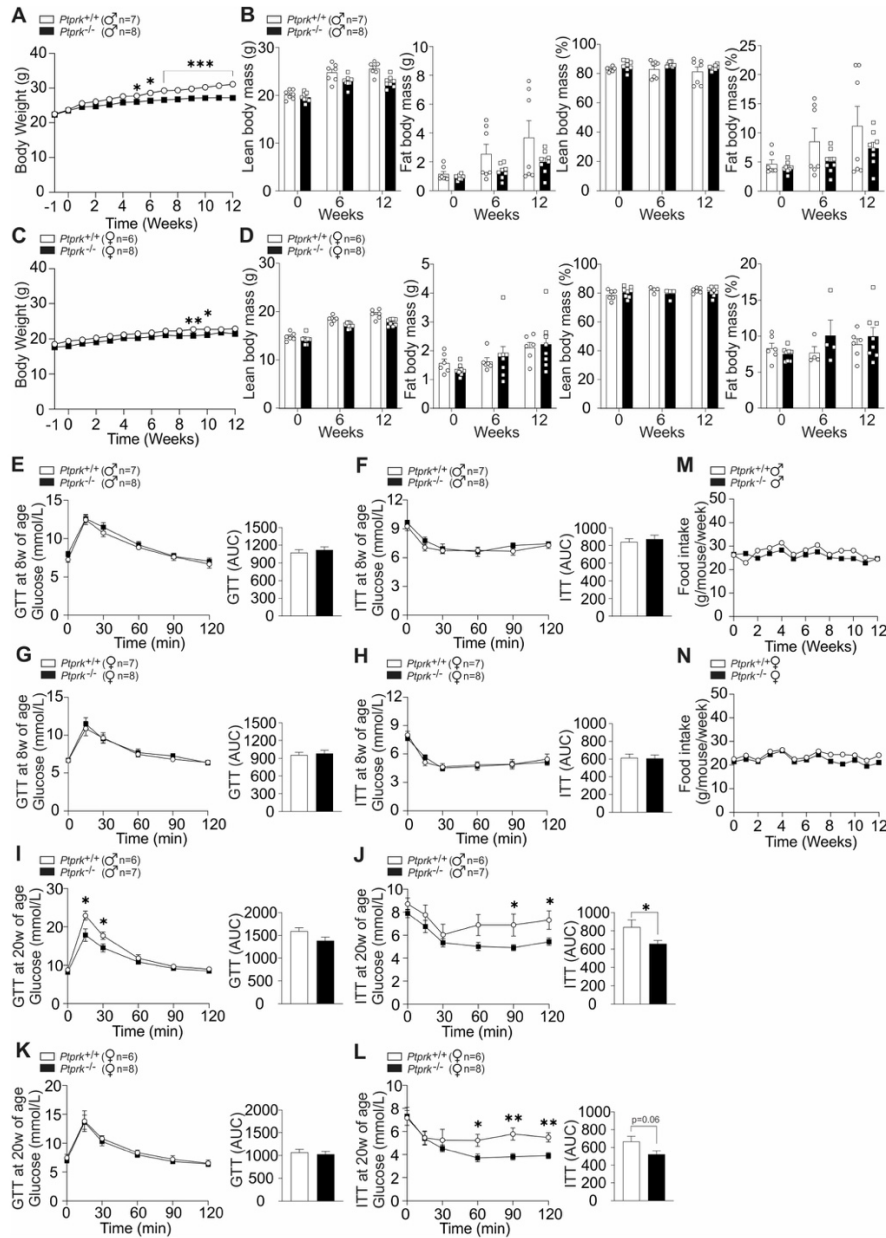
Supplementary Figure 1: Comprehensive liver proteomics, pathway enrichment, and receptor PTPs expression in different hepatic cells.

(A) Heat map displaying the hepatic proteome profile. (B) Proteomic KEGG pathway enrichment analysis comparing steatosis and healthy livers. (C) Proteomic KEGG pathway enrichment analysis comparing NASH and healthy livers. (D) Proteomic KEGG pathway enrichment analysis comparing NASH and steatosis. (E) Data extracted from GSE192740 showing UMAPs with distinct cell clusters identified in the liver and the distribution of various receptor PTPs across parenchymal and non-parenchymal hepatic cells.



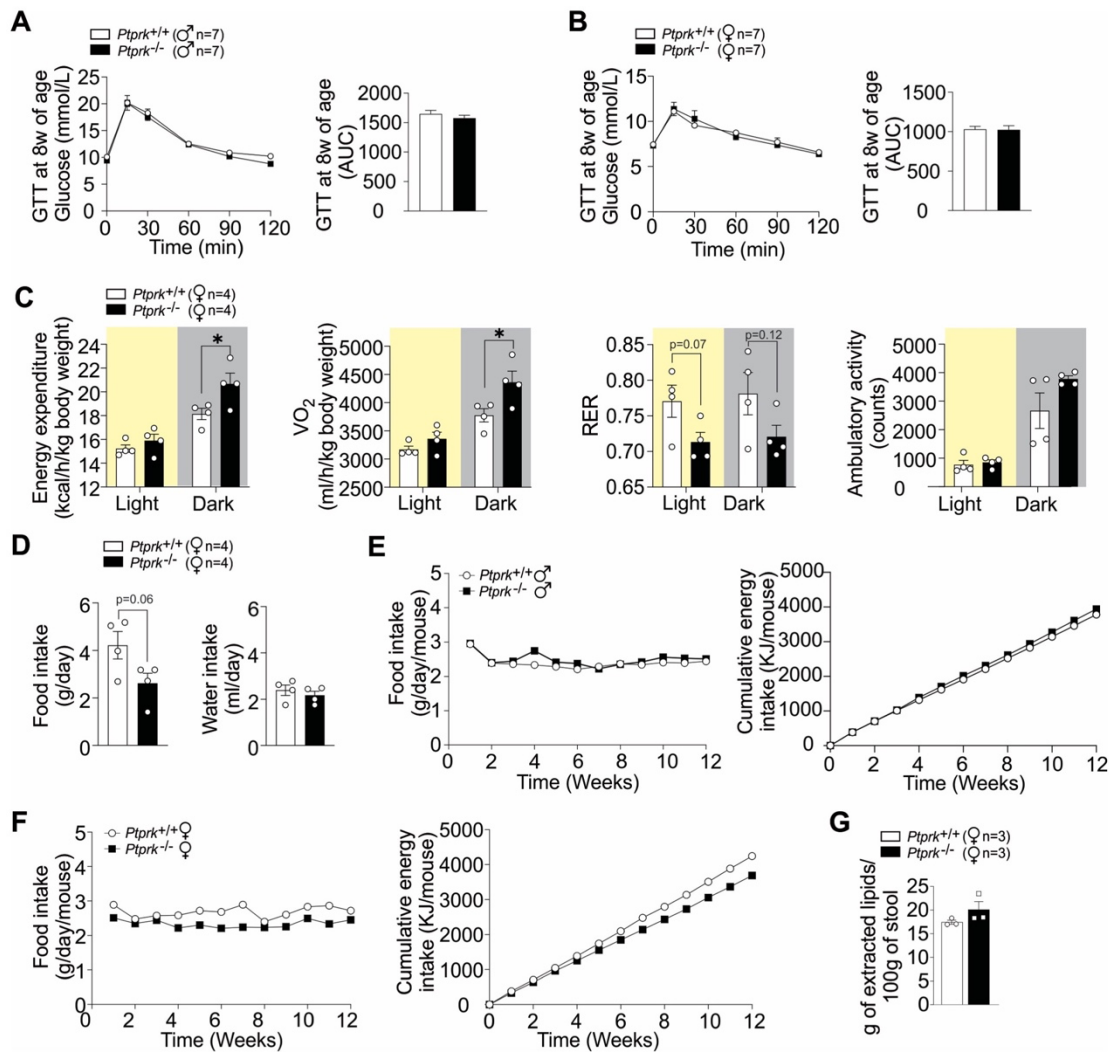
Supplementary Figure 2: Insulin or cytokine treatment does not affect PTPRK expression and culture of primary hepatocytes enhances Notch2 expression.

(A) Immunoblot analysis of PTPRK expression in mouse primary hepatocytes cultured over time treated with insulin as indicated. (B) Immunoblot analyses of PTPRK expression in mouse primary hepatocytes with acute (4h) and chronic (24h) TNF α treatment. (C) Immunoblot analyses of PTPRK expression in mouse primary hepatocytes with acute (4h) and chronic (24h) IL6 treatment. (D) Immunoblot analyses of PTPRK expression in mouse primary hepatocytes with acute (4h) and chronic (24h) IFN γ treatment. (E) Immunoblot analyses of NOTCH2 expression in mouse primary hepatocytes over time in culture. The presented data represents the average of different independent experiments and are expressed as mean \pm SEM. Statistical significance is indicated as ** $p < 0.05$, ** $p < 0.01$, *** $p < 0.001$.



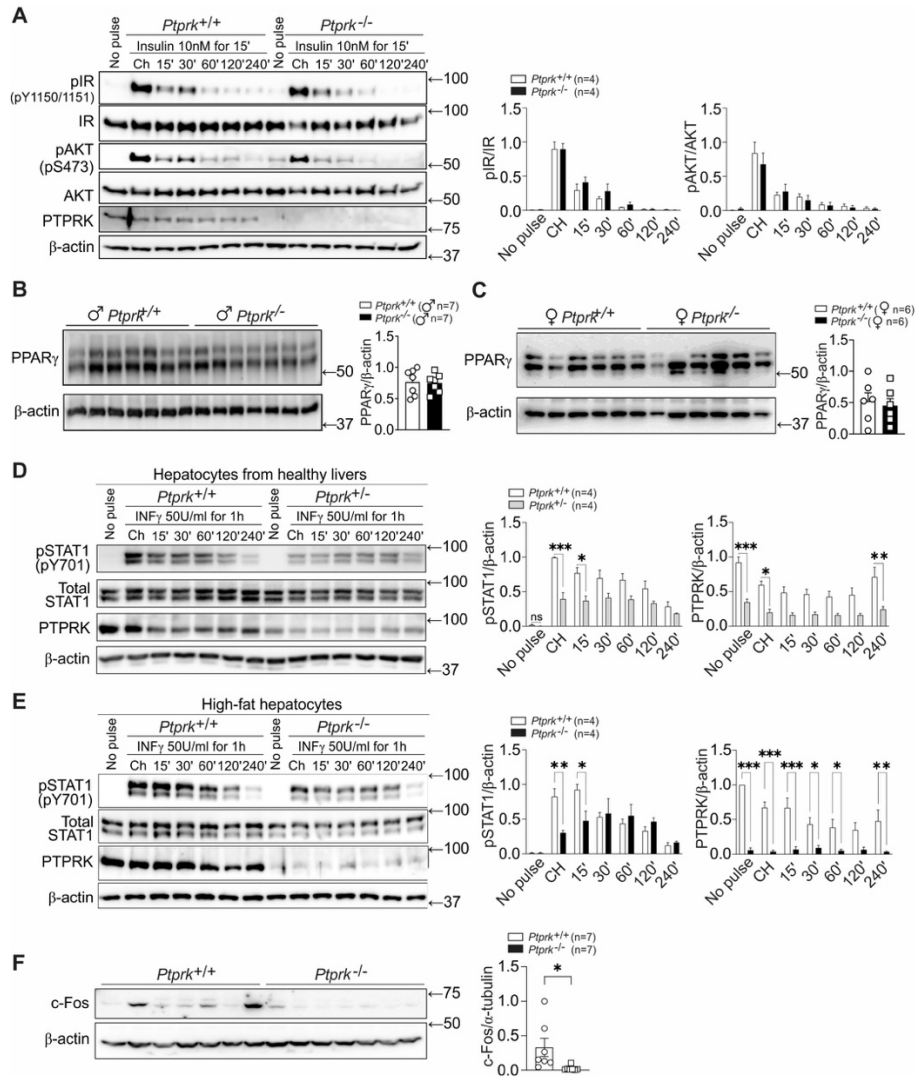
Supplementary Figure 3: Metabolic phenotype shows minor differences in body weight and composition in *Ptpdk*^{-/-} and *Ptpdk*^{+/+} mice fed a chow diet.

(A) Male (♂) *Ptpdk*^{-/-} and *Ptpdk*^{+/+} C57BL6N mice aged eight weeks, continuously fed a chow diet for additional 12 weeks, and body weight was measured weekly. (B) Body composition in male mice. (C) Female (♀) *Ptpdk*^{+/+} and *Ptpdk*^{-/-} C57BL6N mice aged eight weeks, continuously fed a chow diet for 12 weeks, and body weight was measured weekly. (D) Body composition of female mice. (E) Glucose tolerance test in male mice at 8 weeks of age. (F) Insulin tolerance test in male mice at 8 weeks of age. (G) Glucose tolerance test in female mice at 8 weeks of age. (H) Insulin tolerance test in female mice at 8 weeks of age. (I) Glucose tolerance test in male mice at 20 weeks of age. (J) Insulin tolerance test in male mice at 20 weeks of age. (K) Glucose tolerance test in female mice at 20 weeks of age. (L) Insulin tolerance test in female mice at 20 weeks of age. (M) Food intake in male mice. (N) Food intake in female mice. The presented data represent the average of independent experiments and are expressed as mean±SEM. Statistical significance is indicated as **p*<0.05, ***p*<0.01, ****p*<0.001.



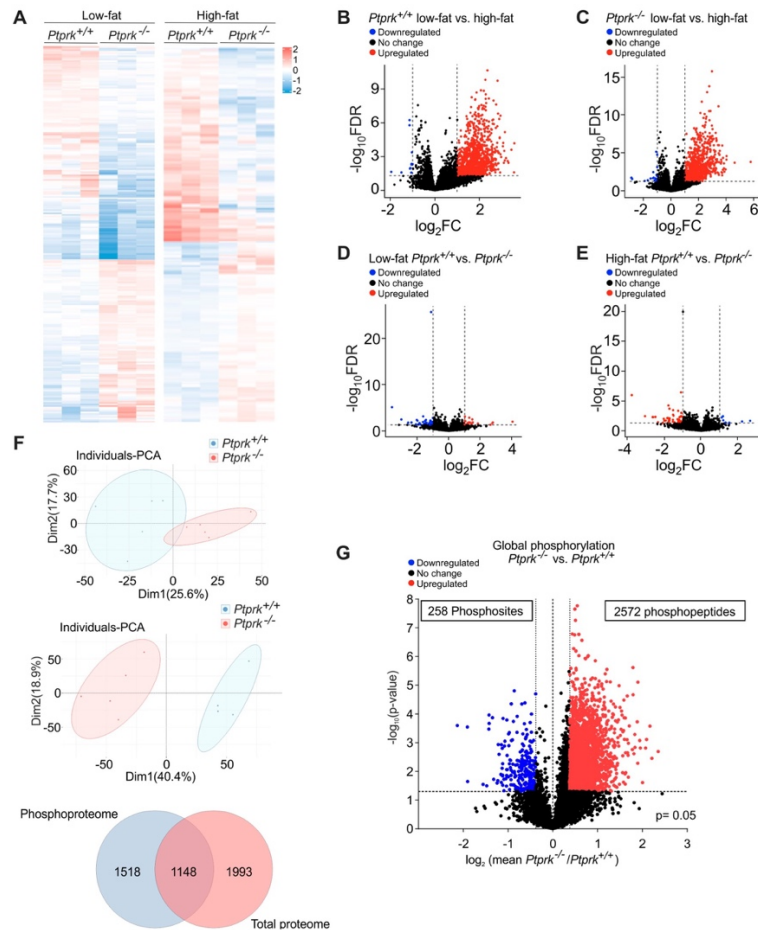
Supplementary Figure 4: Metabolic assessments in *Ptpdk*^{-/-} and *Ptpdk*^{+/+} mice fed a high-fat, high-fructose, high-cholesterol diet.

(A, B) Glucose tolerance test performed in males at 8 weeks of age (before the HFHFHCD feeding). (C) Energy expenditure, oxygen consumption (VO_2), respiratory exchange ratio ($RER = VCO_2/VO_2$) and ambulatory activity measurements in female *Ptpdk*^{+/+} and *Ptpdk*^{-/-} mice after high-fat, high-fructose, high-cholesterol diet (HFHFHCD) feeding for 8 weeks. (D) Daily food and water intake. (E) Average food intake and cumulative energy intake analyses in males HFHFHCD. (F) Average food intake and cumulative energy intake analyses in females HFHFHCD. (G) Lipid extraction from stool samples collected over three consecutive days before the end of the 12-week HFHFHCD feeding experimental period. The presented data represent the average of independent experiments and is expressed as mean \pm SEM. Statistical significance is indicated as $*p < 0.05$.



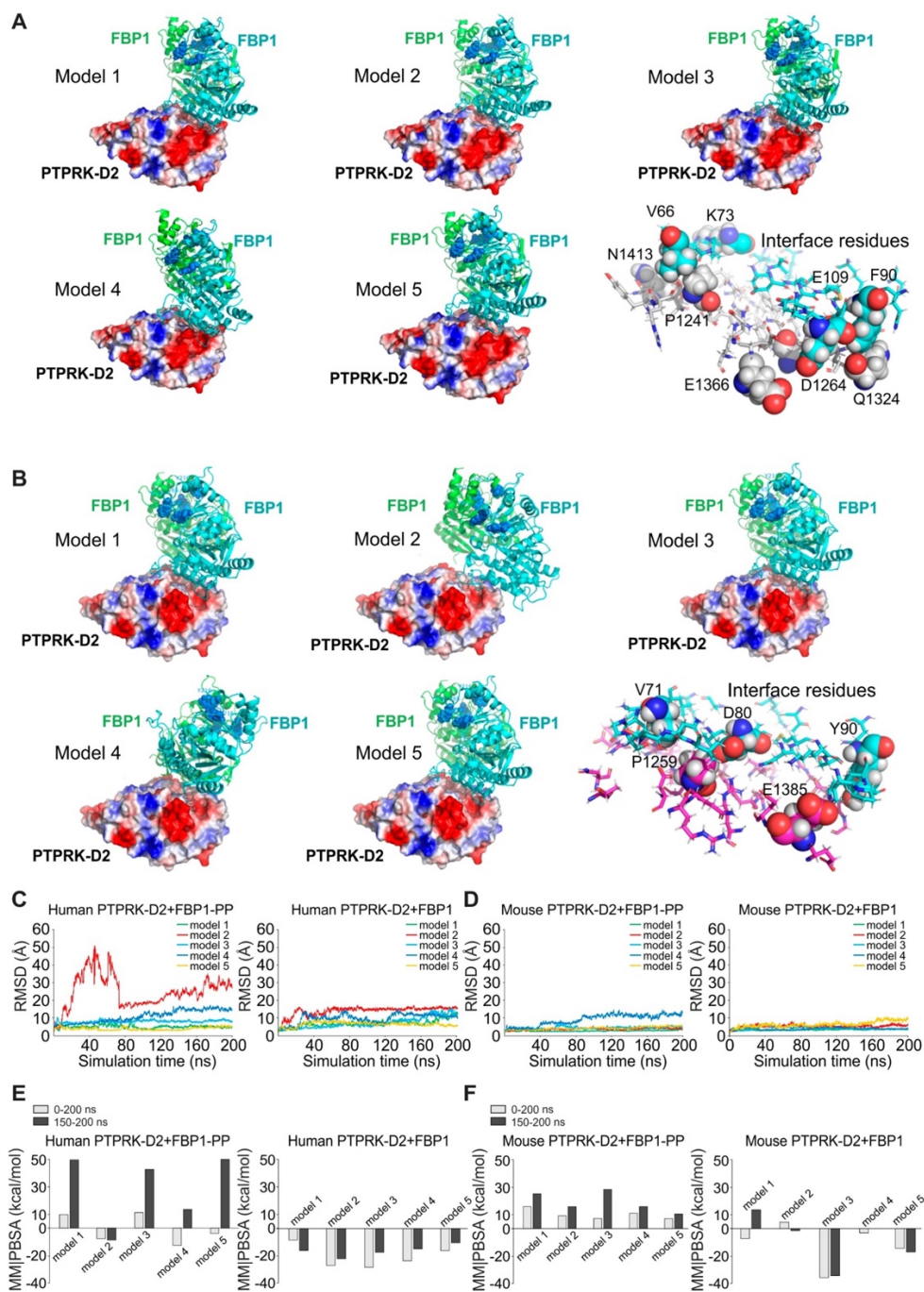
Supplementary Figure 5: Effect of PTPRK on insulin signalling, IFN γ -induced STAT1 activation and hepatic c-Fos expression.

(A) Immunoblot analysis of hepatocytes isolated from *Ptprk*^{-/-}, *Ptprk*^{+/-}, and *Ptprk*^{+/+} mice cultured overnight and subjected to pulse and chase after insulin treatment. The analysis reveals that PTPRK deletion does not significantly affect hepatocyte insulin signalling, as demonstrated by pIR, IR, pAKT, AKT, and PTPRK levels in *Ptprk*^{-/-} and *Ptprk*^{+/+} hepatocytes isolated from healthy male mice at 8 weeks of age following a 15-min exposure to 10nM of insulin, chase (Ch). (B, C) Visceral epididymal (males, B) and uterine (females, C) white adipose tissues were collected for immunoblot analysis of PPAR γ . (D) Immunoblot analysis showing lower PTPRK levels associated with decreased pSTAT1 activation in response to IFN γ in *Ptprk*^{+/-} and *Ptprk*^{+/+} hepatocytes after 1h exposure to 50 U/ml IFN γ . (E) Immunoblot analysis of IFN γ -induced STAT1 activation in *Ptprk*^{-/-} and *Ptprk*^{+/+} hepatocytes with high-fat content isolated from steatotic livers of male mice at 14 weeks of age following a 1-hour exposure to 50 U/ml IFN γ . (F) c-Fos expression was assessed by immunoblot analysis in livers from female *Ptprk*^{-/-} and *Ptprk*^{+/+} mice fed a high-fat, high-fructose, high-cholesterol diet for 12 weeks. The presented data represent the average of independent experiments and are expressed as mean \pm SEM. Statistical significance is indicated as * p <0.05, ** p <0.01, *** p <0.001.



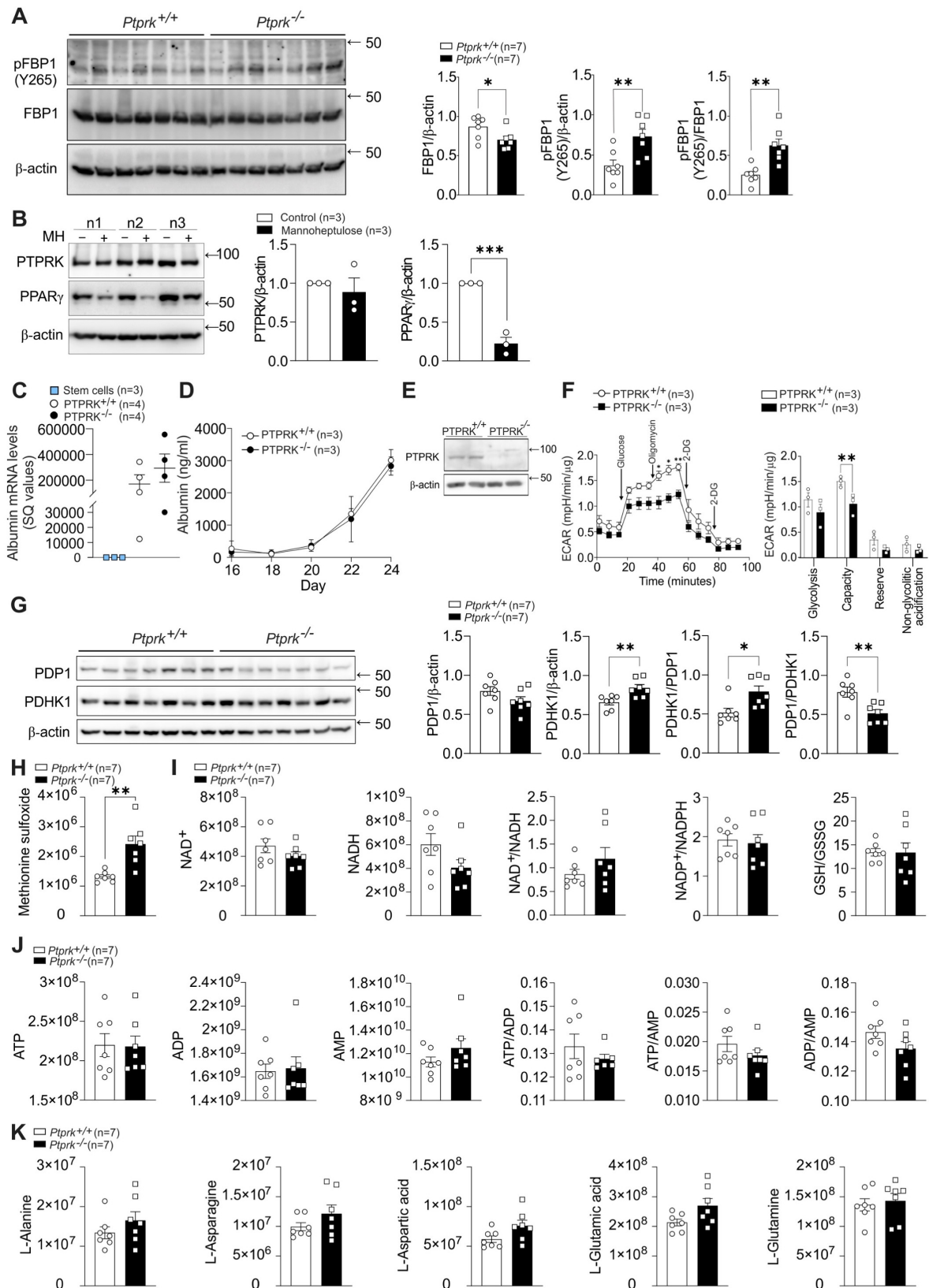
Supplementary Figure 6: Transcriptome, proteome, and protein phosphorylation assays in primary mouse hepatocytes isolated from *Ptprk*^{-/-} and *Ptprk*^{+/+} mice.

(A) RNA-Seq heatmap showing alterations in mRNA expression in hepatocytes with low- and high-fat content. (B) Volcano plot showing the quantification of transcripts in high-fat and low-fat *Ptprk*^{+/+} hepatocytes. (C) Volcano plot showing the quantification of transcripts in high-fat and low-fat *Ptprk*^{-/-} hepatocytes. (D) Volcano plot displaying the quantification of transcripts between *Ptprk*^{-/-} and *Ptprk*^{+/+} hepatocytes with low fat content. (E) Volcano plot displaying the quantification of transcripts between *Ptprk*^{-/-} and *Ptprk*^{+/+} hepatocytes with high-fat content. (F) PCA analysis depicting changes in the total proteome (top part) and phosphoproteome (middle part) in *Ptprk*^{-/-} and *Ptprk*^{+/+} hepatocytes. Principal component analysis (PCA) examination revealed that the PCA scores for PC1 (Dim1) and PC2 (Dim2) generated a biplot that segregated into two distinct groups. PC1 and PC2 collectively explained 43.3% of the variability between *Ptprk*^{-/-} and *Ptprk*^{+/+} samples, with PC1 accounting for 25.6% and PC2 for 17.7% of the variance, respectively. A similar analysis for the phosphoproteomic data showed a more pronounced difference, with PCA scores for PC1 (Dim1) and PC2 (Dim2) producing a biplot that distinctly separated two groups. In this case, PC1 and PC2 together explained 59.3% of the variability between *Ptprk*^{-/-} and *Ptprk*^{+/+} samples, with PC1 contributing 40.4% and PC2 contributing 18.9% of the variance. One group comprised *Ptprk*^{+/+} hepatocytes, while the other group consisted of *Ptprk*^{-/-} hepatocytes, both showing strong alignment along principal component 2 (PC2). Venn diagram illustrating proteins identified in the phosphoproteome and total proteome (bottom part). (G) Volcano plot showing the quantification of phosphosites between *Ptprk*^{-/-} and *Ptprk*^{+/+} hepatocytes with high-fat content.



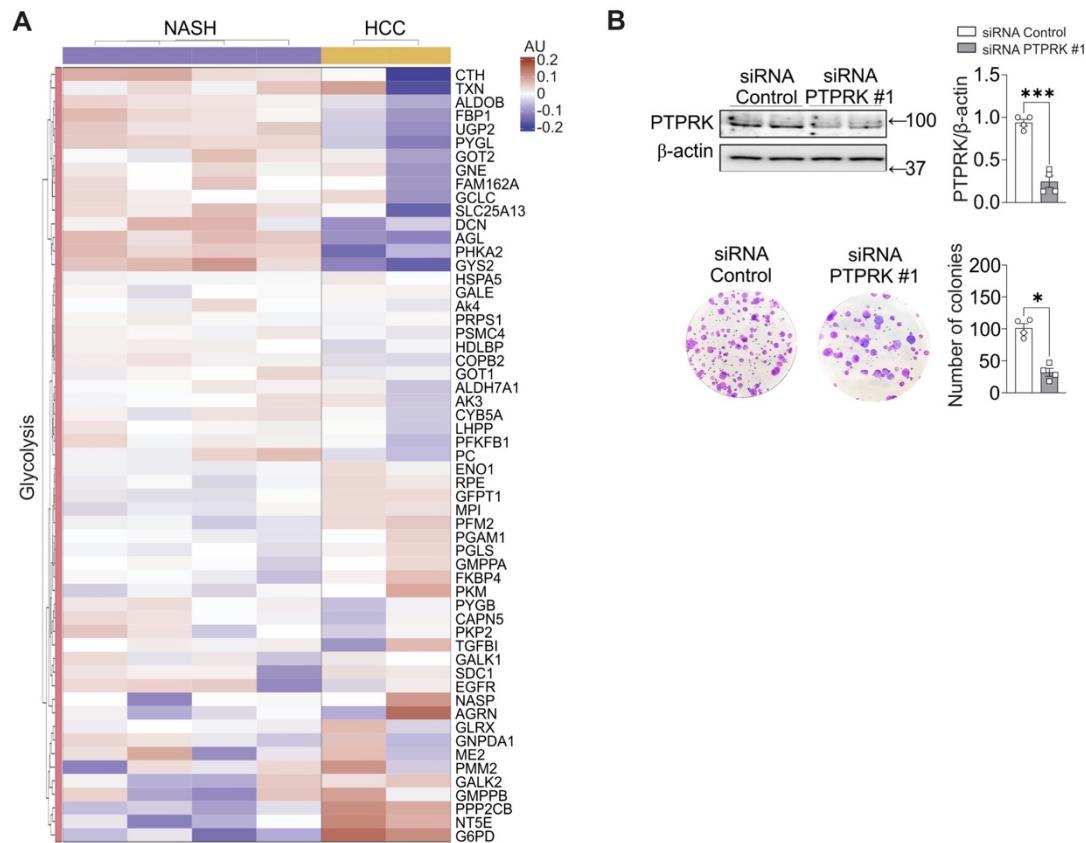
Supplementary Figure 7: Computational modelling of the interaction between phosphorylated FBP1 dimer (PP-FBP1) and PTPRK-D2 non-catalytic domain.

(A-B) The images show the surface of the human (A) and mouse (B) PTPRK-D2 non-catalytic domain and with 5 different models of the interaction between PTPRK and FBP1 (backbone of dimer are shown in green and cyan for each monomer) and the predicted interface residues participating in the PTPRK-FBP1 interaction. The colour coding represents the hydrophobicity of the amino acid side chains on the surface. (C-D) The RMSD values in Å for the five interaction models were calculated during the 200-ns MD simulation for human PTPRK (C) and mouse PTPRK (D). (E-F) The solvation binding energy (MM|PBSA, kcal/mol) values for the time intervals of 0-200 ns and the final 150-200 ns of FBP1-PTPRK D2 domain interaction simulation for phosphorylated FBP1 (PP-FBP1, pY265 and pY245) and non-phosphorylated FBP1 are presented for human (E) and mouse (F).



Supplementary Figure 8: Metabolic profiling of *PTPRK*^{-/-} and *PTPRK*^{+/+} human stem cell-derived hepatocyte-like cells and metabolite analysis in livers from *Ptprk*^{-/-} and *Ptprk*^{+/+} mice. (A) Liver samples from *Ptprk*^{-/-} and *Ptprk*^{+/+} female mice fed a 12-week high-fat, high-fructose, high-cholesterol diet (HFHFHCD) were extracted and processed for immunoblot analysis to evaluate the expression of pFBP1 (Y265) and total FBP1 levels. (B) Primary mouse hepatocytes were exposed to mannoheptulose (MH) as indicated and

PTPRK/PPAR γ assessed by immunoblot. (C) Human embryonic stem cells CRISPR-Cas12a-edited to delete PTPRK were differentiated into hepatocyte-like cells. Albumin mRNA levels were measured in stem cells, *Ptprk*^{-/-} and *Ptprk*^{+/+} hepatocyte-like cells. (D) Albumin levels were quantified over the course of the differentiation process using enzyme-linked immunosorbent assay (ELISA). (E) Immunoblot analysis was performed after differentiation into hepatocyte-like cells. (F) A glycolysis stress test was conducted in *PTPRK*^{-/-} and *PTPRK*^{+/+} hepatocyte-like cells. Real-time measurements of the extracellular acidification rate (ECAR) in response to glycolytic modulators were recorded. (G) Liver samples from *Ptprk*^{-/-} and *Ptprk*^{+/+} female mice fed a 12-weeks HFHFHCD were extracted and processed for immunoblot analysis to evaluate the expression of PDP1 and PDHK1. (F-K) Livers were harvested from *Ptprk*^{-/-} and *Ptprk*^{+/+} female mice fed a 12-week HFHFHCD and metabolite analysis was conducted using mass spectrometry: (H) methionine sulfoxide, (I) redox status indicators NAD⁺, NADH, NADP⁺/NADPH and reduced glutathione (GSH) to oxidized glutathione (GSSG) ratios (J) energy status indicators ATP, ADP, AMP, and their ratios and (K) levels of amino acids. Metabolites are presented as raw abundances corrected for sample weight. The presented data represent the average of independent experiments and are expressed as mean \pm SEM. Statistical significance is indicated as * p <0.05, ** p <0.01, *** p <0.001.



Supplementary Figure 9: Glycolysis-related protein expression heatmaps in NASH and HCC human liver samples, and PTPRK knockdown in hepatoma cell colony formation. (A) Heatmaps were generated to illustrate the expression of proteins involved in glycolysis/gluconeogenesis in human liver samples from individuals with NASH or HCC. (B) Huh6 cells were transfected with siRNA targeting PTPRK or siRNA control. Transfection efficiency was confirmed by immunoblot analysis, and colony-forming capacity was assessed using crystal violet staining for colony number counting. The presented data are expressed as mean±SEM, with statistical significance indicated as * $p < 0.05$, *** $p < 0.001$.

ID	Biopsy health status	Age	Weight (kg)	Height (cm)	BMI (kg/m ²)	Type 2 diabetes	Gender	Experiment
CHR01	Healthy liver	80	46	175	15	No	M	MS/IHC
CHR02	Healthy liver	66	62	150	28	No	F	MS/IHC
CHR03	Healthy liver	28	66	170	23	No	F	IHC
CHR04	Healthy liver	63	66	165	24	No	F	MS/IHC
CHR08	Steatosis	53	86	185	25	Yes	F	MS/IHC
CHR09	Steatosis	39	80	158	32	No	F	MS/IHC
CHR10	Steatosis	56	67	173	22	No	M	MS/IHC
CHR11	Steatosis	36	82	160	32	No	F	MS/IHC
CHR12	Steatosis	61	76	159	30	No	F	IHC
CHR13	Steatosis	68	115	168	41	Yes	M	IHC
CHR14	NASH/Cirrhosis	61	113	179	35	Yes	M	MS/IHC
CHR16	NASH/Cirrhosis	46	79	156	32	No	F	MS/IHC
CHR17	NASH/Cirrhosis	48	76	160	30	No	M	MS/IHC
CHR18	NASH/Cirrhosis	60	80	149	36	Yes	F	MS/IHC
CHR19	NASH	46	80	157	32	Yes	F	MS
CHR20	NASH	45	85	156	35	Yes	F	MS
CHR05	HCC	83	79	175	26	No	M	MS
CHR06	HCC	76	76	165	28	No	M	MS
CHR07	HCC	43	55	170	19	No	M	MS

Supplementary table 1: Clinical and demographic characteristics of patients from whom liver biopsies were collected and used for mass spectrometry (MS) or PTPRK immunohistochemistry (IHC) analysis shown in Figure 1.

siRNA	Source or reference	Identifiers	Sense (5'→3')	Antisense (5'→3')
siRNA PTPRK #1	Ambion by Life Technologies	s11559	CCAGUAGCCCAG ACUAAGAtt	UCUUAGUCUGGG CUACUGGta
siRNA PTPRK #2	Ambion by Life Technologies	s11558	CAGCUAUAGCAG UAUAAGAtt	UCUUAUACUGCUA UAGCUGat
siRNA Control	Quiagen	1027281	-	-

Supplementary table 2: List of siRNAs used for RNA interference in the present study.

Antibody	Designation	Source or reference	Identifiers	Additional information
β -actin	Mouse monoclonal anti-beta-actin	Sigma-Aldrich	Cat# A1978	Western blot 1:5000
GAPDH	Rabbit polyclonal anti-glyceraldehyde-3-phosphate dehydrogenase	R&D Systems	Cat# 2275-PC-100	Western blot 1:5000
α -tubulin	Mouse monoclonal anti-alpha-tubulin	Sigma-Aldrich	Cat# T5168	Western blot 1:5000
Vinculin	Rabbit polyclonal anti-vinculin	Cell Signaling Technology	Cat# 4650	Western blot 1:1000
pY	Mouse monoclonal anti-phospho-tyrosine antibody	Cell Signaling Technology	Cat# 9411	IP 1:50 Western blot 1:1000
PTPRK	Human monoclonal anti-PTPRK	Fearnley et al. 2019, Kindly provided by Hayley Sharpe	2 .H4	Western blot 1:1000
PTPRK	Rabbit polyclonal anti-PTPRK	Thermo Fisher Scientific	Cat# PA5-104089	IHC 1:100
PPAR γ	Rabbit monoclonal anti- PPAR γ	Cell Signaling Technology	Cat# 2443	Western blot 1:500
pIR	Rabbit monoclonal anti-phospho-IGF-I Receptor β (Tyr1135/1136)/Insulin Receptor β (Tyr1150/1151)	Cell Signaling Technology	Cat# 3024S	Western blot 1:500
IR	Rabbit monoclonal anti-Insulin Receptor β	Cell Signaling Technology	Cat# 3025	Western blot 1:1000
pAKT	Rabbit monoclonal anti-phospho-AKT (Ser473)	Cell Signaling Technology	Cat# 4060	Western blot 1:1000
AKT	Mouse monoclonal anti-AKT (pan)	Cell Signaling Technology	Cat# 2920S	Western blot 1:1000
ACC	Mouse monoclonal anti-acetyl CoA carboxylase	Cell Signaling Technology	Cat# 3676S	Western blot 1:1000
FASN	Rabbit monoclonal anti-fatty acid synthase	Cell Signaling Technology	Cat# 3180S	Western blot 1:1000
SREBP1	Mouse monoclonal anti-sterol regulatory element binding protein 1	Santa Cruz Biotechnology	Cat# sc-13551	Western blot 1:1000
ChREBP1 α	Rabbit polyclonal anti-Carbohydrate-responsive element-binding protein alpha	Cell Signaling Technology	Cat# 58069	Western blot 1:1000
pFBP1 (Y265)	Rabbit polyclonal anti-Phospho-fructose 1,6 biphosphatase 1 (Tyr265)	Thermo Fisher Scientific	Cat# PA5-105335	Western blot 1:1000
FBP1	Rabbit polyclonal anti-fructose 1,6 biphosphatase 1	Cell Signaling Technology	Cat# 59172	Western blot 1:1000
PDP1	Rabbit monoclonal anti-pyruvate dehydrogenase phosphatase 1	Cell Signaling Technology	Cat# 65575S	Western blot 1:1000
PDHK1	Rabbit monoclonal anti-pyruvate dehydrogenase kinase 1	Cell Signaling Technology	Cat# 3820S	Western blot 1:1000
c-Fos	Rabbit polyclonal anti-protein c-Fos	Cell Signaling Technology	Cat# 4384S	Western blot 1:1000
Notch2	Rabbit monoclonal anti-Neurogenic locus notch homolog protein 2	Cell Signaling Technology	Cat# 5732S	Western blot 1:1000
HIF-2 α	Rabbit monoclonal anti-Hypoxia-inducible factor 2 alpha	Cell Signaling Technology	Cat# 57921S	Western blot 1:500

Supplementary table 3: Antibodies used in the present study.

Gene name	qPCR Fw	qPCR Rv	STD Fw	STD Rv
Tnf	AGGCACTCCCC CAAAAGATG	TGAGGGTCTGGG CCATAGAA	ATGAGCACAGA AAGCATGATC	TACAGGCTTGT CACTCGAATT
Ppar γ 1	CCAAGAATACCA AAGTGCGATCA	AAAACCCTTGCA TCCTTCACAA	GCTCCAAGAAT ACCAAAGTGCG A	AACCTGATGGC ATTGTGAGACA
Ppar γ 2	TGCCTATGAGCA CTTCACAAG	TCTACTTTGATC GCACTTTGGTA	AGCATGGTGCC TTCGCTGAT	GCCCAAACCTG ATGGCATTGTG
Cyp7a1	TAAGGAGAAGG AAAGTAGGTGAA C	CCAAATGCCTTC GCAGAAGTAG	TGGAATAAGGA GAAGGAAAGTA GG	TCCAAATGCCTT CGCAGAAGTA
Gapdh	AGTTCAACGGCA CAGTCAAG	TACTCAGCACCA GCATCACC	ATGACTCTACC CACGGCAAG	TGTGAGGGAGA TGCTCAGTG
Fasn	CACAGTGCTCAA AGGACATGCC	CACCAGGTGTAG TGCCTTCCTC	ACTTCCTCTGG GATGTGCCT	GTCAGCACTGC TCTCGTTGA
Pck1	GCAGTGAGGAA GTTCTGTGGA	GTGAGAGCCAGC CAACAGT	GCTGCATAACG GTCTGGACT	ATACATGGTGC GGCCTTTCAT
Cd36	TAATGGCACAGA CGCAGC	GGTTGTCTGGAT TCTGGAGGG	TAATGGCACAG ACGCAGC	ACATCACCCT CCAATCCCA
Cpt1 α	GCTGATGACGG CTATGGTGT	AAAGCGGTGTGA GTCTGTCT	CCACAACAACG GCAGAGCA	TCAGGAGCAAC ACCTATTCATTT G
Scd1	TGCCGTGGGCG AGGG	ACACCCCGATAG CAATATCCA	TGATGTTCCAG AGGAGGTACTA CA	AATGCATCATT ACACCCCGA
Ptprk	TCGTGATTGGCT TCGGG	CCAGCATTGACC TCCACA	TGAAGGAGAAT GACACCCAC	TCTGAAAGAGG CAGCAAATCT
Acly	TTCGTCAAACAG CACTTCC	ATTTGGCTTCTT GGAGGTG	ACACCATCATCT GTGCTCGG	ATCCCAGGGGT GACGATACA
Acaca(Acc)	AGCCAGAAGGG ACAGTAGAA	CTCAGCCAAGCG GATGTAAA	GCGCTTACATT GTGGATGGC	AAGCCTTCACT GTGCCTTCA
Alb(human)	GAAAAGTGGGC AGCAAATGT	GGTTCAGGACCA CGGATAGA	GAGCAGCTTGG AGAGTACAA	GTTTCAGCATT AACTCTTT

Supplementary table 4: Primer sequences used for RT-PCR experiments.